Magnetism and half-metallicity of some Cr-based alloys and their potential for application in spintronic devices

by

Yong Liu, S. K. Bose and J. Kudrnovský

reprinted from

WORLD JOURNAL OF ENGINEERING

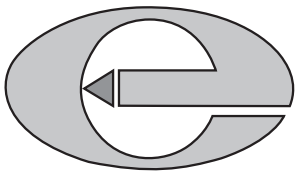

VOLUME 9 NUMBER 2 2012

MULTI-SCIENCE PUBLISHING COMPANY LTD.

World Journal of Engineering 9(2) (2012) 125-132

World Journal of
Engineering

Magnetism and half-metallicity of some Cr-based alloys and their potential for application in spintronic devices

Yong Liu[1], S. K. Bose[2,*] and J. Kudrnovský[3]

[1]College of Science, Yanshan University, Qinhuangdao, Hebei, 066004, China
[2]Physics Department, Brock University, St. Catharines, Ontario L2S 3A1, Canada
[3]Institute of Physics, Academy of the Sciences of the Czech Republic, Na Slovance 2, 182 21 Prague 8, Czech Republic
**E-mail: sbose@brocku.ca*

(Received 12 September 2011; accepted 21 November 2011)

Abstract

We present results of the exchange interactions and Curie temperatures in some Cr-based chalcogenides and pnictides. The calculations are performed mostly for Zinc Blende (ZB) structure with the lattice parameter varying between 5.45 and 6.6 Å, appropriate for some typical II–VI and III–V semiconducting substrates. Electronic structure is calculated via the linear muffin-tin-orbitals method and disorder effects, when appropriate, are taken into account via the coherent potential approximation. Calculated exchange interactions are used to estimate the Curie temperature by employing the mean-field and the random phase approximations. For CrTe we compare the results of the ZB and Rock-Salt (RS) structures.

Key words**:** *Curie temperature, Linear Muffin-Tin Orbitals (LMTO), Coherent Potential Approximation (CPA), Full Potential Linear Augmented Plane Wave (FP-LAPW)*

1. Introduction

Half-metallic (HM) ferromagnetism with relatively high Curie temperatures T_c (room temperatures and above) is an ideal characteristic of materials with potential for application in spintronic devices. Understandably, then, considerable theoretical and experimental efforts have been devoted in recent years to the search for such materials. Cr-doped dilute magnetic semiconductorsand some Cr-based alloys in ZB structure have been predicted to exhibit HM ferromagnetism (Saito *et al*., 2003; Galanakis and Mavropoulos, 2003). Akinaga *et al*. have grown ferromagnetic (FM) ZB thin films, which showed T_c in excess of 400 K (Akinaga *et al*., 2000). Thin films of CrSb grown by solid-source molecular beam epitaxy on GaAs, (Al, Ga)Sb, and GaSb have been found to be of ZB structure and FM with T_c higher than 400 K (Zhao *et al.,* 2001). Recently, Deng *et al*. were successful in increasing the thickness of ZB-CrSb films to ~3 nm by molecular beam epitaxy using (In, Ga)As buffer layers, and Li *et al*. were able to grow ~4 nm thick ZB-CrSb films on NaCl (100) substrates (Deng *et al*., 2006). Sreenivasan *et al*. and Bi *et al*. have reported growing ~5 nm thick films of ZB CrTe using molecular beam epitaxy on GaAs (100) substrate via a ZnTe buffer layer (Sreenivasan *et al*., 2008). Their measurements of temperature-dependent remanent-magnetization indicate a Curie temperature

ISSN:1708-5284

of ~100 K in these films. Our own recent theoretical searches have identified some Cr-based chalcogenides and pnictides (Liu *et al*., 2010; Bose and Kudrnovský, 2010) as holding promise in this regard. We will discuss some of the highlights of these calculations.

2. Method

We have carried out electronic structure calculations using the tight-binding linear muffin-tin orbital (TB-LMTO) (Andersen and Jepsen, 1984) and the coherent potential approximation (CPA) (Kudrnovský and Drchal, 1990). The exchange-correlation potential for this local spin density (LSD) functional method was most often chosen to be the one given by Vosko, Wilk and Nusair (Vosko *et al*., 1980). Electronic and magnetic properties of CrX (X = As, Sb, S, Se and Te) and $CrAs_{50}X_{50}$ (X = Sb, S, Se and Te) were calculated for lattice parameters varying between 5.45 and 6.6 Å, appropriate for some typical II–VI and III–V semiconducting substrates. In our LMTO calculation we optimize the ASA (atomic sphere approximation) errors by including empty spheres in the unit cell.

For several cases, we have checked the accuracy of the LMTO-ASA electronic structures against the full-potential LMTO results (Savrasov and Savrasov, 1992) and found them to be satisfactory. For the mixed alloys $CrAs_{50}X_{50}$ (X = Sb, S, Se and Te), the As-sublattice of the ZB CrAs structure is assumed to be randomly occupied by an equal concentration of As and X atoms. The disorder in this sublattice is treated under the coherent potential approximation (CPA) (Kudrnovský and Drchal, 1990). For CrTe, calculations were done for three structures: NiAs-type hexagonal (NA), ZB and RS. For these cases we also use the full-potential linear augmented plane-wave (FP-LAPW) method (WIEN2k code) (Blaha *et al*., 2001).

The total (band) energy is mapped into a Heisenberg spin-Hamiltonian form:

$$H_{eff} = -\sum_{i,j} J_{ij}\, e_i\, e_j \qquad (1)$$

where i, j are site indices, e_i is the unit vector pointing along the direction of the local magnetic moment at site i, and J_{ij} is the exchange interaction between the moments at sites i and j. Using multiple-scattering formalism, the exchange integral in Eq. (1) can be shown to be given by

$$J_{ij} = (1/4\pi)\, \mathrm{Im} \int \mathrm{tr}_L\, [\Delta_i(z) g_{ij}^{\uparrow}(z) \Delta_j(z) g_{ji}^{\downarrow}]\, dz\,, \qquad (2)$$

where $z = E + i$ represents the complex energy variable, $L = (l, m)$, and $\Delta_i(z) = P_i^{\uparrow}(z) - P_i^{\downarrow}(z)$, spin electrons at site 'i' representing the difference in the potential functions for the up and down. In the present work $g_{ij}^{\delta}(z)(\delta=\uparrow,\downarrow)$ represents the matrix elements of the Green's function of the medium for the up and down spin electrons. The quantity J_{ij} given by Eq. (2) includes direct-, indirect-, double-exchange and superexchange interactions, which are often treated separately in model calculations. The negative sign in Eq. (1) implies that positive and negative values of J_{ij} are to be interpreted as representing FM and AFM interactions, respectively. One can obtain the Curie temperature T_c in mean field approximation (MFA) from

$$k_B T_c^{MFA} = \frac{2}{3} \sum_{i \neq 0} J_{0i}^{Cr,Cr} \qquad (3)$$

where the sum extends over all the neighboring shells. An improved description of finite-temperature magnetism is provided by the random phase approximation (RPA), with T_c given by

$$\left(k_B T_c^{RPA}\right)^{-1} = \frac{3}{2} \frac{1}{N} \sum_{i \neq 0} \left[J_{0i}^{Cr,Cr}(0) - J_{0i}^{Cr,Cr}(q) \right]^{-1} \qquad (4)$$

Here N denotes the order of the translational group applied and $J^{Cr,Cr}(q)$ is the lattice Fourier transform of the real-space exchange integrals $J_{ij}^{Cr,Cr}$. We have calculated the exchange interactions and T_c for both FM reference state and paramagnetic reference state represented by the disordered local moment (DLM) (Heine, 1980) model. The FM results follow from the usual spin-polarized calculations, where self-consistency of charge- and spin-density yields a nonzero magnetization per unit cell. Although we call this the FM result, our procedure does not guarantee that the true ground state of the system is FM, with the magnetic moments of all the unit cells perfectly aligned. This is because we have not explored non-collinear magnetic states, nor all AFM states attainable within the collinear model. Indeed, our results for the exchange interactions in some cases do suggest the ground states being of AFM or complex magnetic nature. For lack of a suitable label, we refer to all spin-polarized calculations giving a nonzero local moment as FM state calculations. Within the Stoner

model, a nonmagnetic state above the Curie temperature T_c would be characterized by the vanishing of the local moments in magnitude. An alternate description of the nonmagnetic state is provided by the DLM model, where the local moments remain nonzero in magnitude above T_c but disorder in magnitude as well as their direction above T_c causes the global magnetic moment to vanish. This model can be considered as a disordered binary alloy problem, and treated within the CPA. Estimates of the exchange interactions and T_c calculated within the DLM model thus portray the reference state as being paramagnetic. Hence, in effect, estimates of T_c based on FM and DLM models can be considered as estimates from below and above, respectively, the magnetic transition (Bose and Kudrnovský, 2010).

3. Results

Our density functional calculations show that half-metallicity as well as ferromagnetism survive in most of these Cr-based chalcogenides and pnictides in ZB structure over a wide range of the lattice parameter. Exceptions occur for the chalcogenides, CrS, CrSe, and CrTe, at lower values of the lattice parameters, where large AFM interactions compete with weaker FM interaction among the Cr-Cr and Cr-chalcogen pairs, suggesting instability of the FM state against AFM or complex magnetic phases. For the pnictides no AFM spin fluctuations are found over a wide range of the lattice parameter, including low values. For details, we refer the readers to our previous publication (Bose and Kudrnovský, 2010, see Table II, in particular).

Electron density of states (DOS) in ZB structure Cr-based binary alloys has been discussed in detail by various authors (Galanakis and Mavropoulos, 2003). Here we present results for some mixed ternary alloys, in particular $CrAs_{50}Sb_{50}$ and $CrAs_{50}Se_{50}$. In Figures 1 and 2 we show the DOS for $CrAs_{50}Sb_{50}$ and $CrAs_{50}Se_{50}$, for lattice parameters above and below the critical values for the HM character. According to Galanakis and Mavropoulos, half-metallicity in ZB CrAs appears between the lattice parameters of 5.45 and 5.65 Å (Galanakis and Mavropoulos 2003). The latter corresponds to the lattice parameter of the GaAs substrate. For CrSb half-metallicity appears at a lattice parameter between 5.65 and 5.87 Å. The mixed alloy $CrAs_{50}Sb_{50}$, as shown in Fig. 1, is not quite HM at the lattice parameter of 5.65 Å, and fully HM at the lattice parameter of 5.76 Å. Replacing Sb with Se in the above alloy, i.e. for $CrAs_{50}Se_{50}$, brings

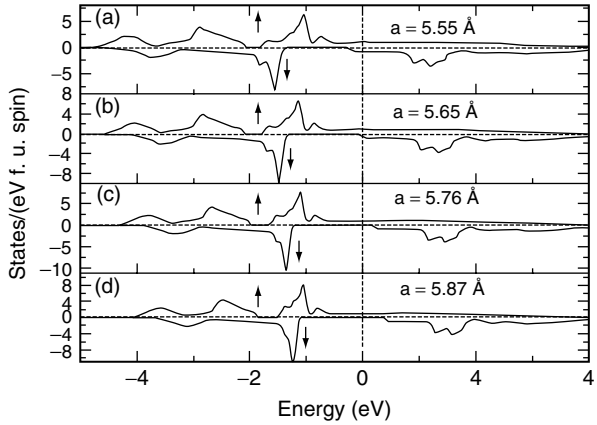

Fig. 1. Spin-resolved densities of states in ZB $CrAs_{50}Sb_{50}$ for lattice parameters. (a) 5.55 Å. (b) 5.65 Å. (c) 5.76 Å. (d) 5.87 Å.

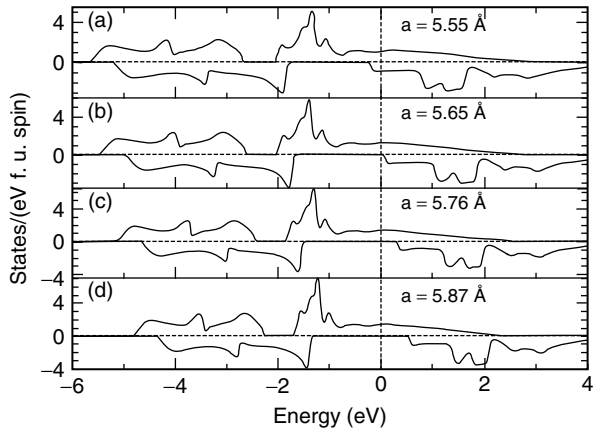

Fig. 2. Spin-resolved densities of states in ZB $CrAs_{50}Se_{50}$ for lattice parameters. (a) 5.55 Å. (b) 5.65 Å. (c) 5.76 Å. (d) 5.87 Å.

the critical lattice parameter down slightly. As shown in Fig. 2, at a lattice parameter of 5.65 Å, $CrAs_{50}Se_{50}$ is HM, although barely so. In our calculation CrS and CrSe are HM at a lattice parameter of 5.65 Å, and not so at a lattice parameter of 5.55 Å. CrTe is not HM at a lattice parameter of 5.76 Å, but at a lattice parameter of 5.87 Å. For both CrS and CrSe the critical value should be close to 5.65 Å, and for CrTe it should be close to 5.87 Å. Note that in general the HM gap is larger in the chalcogenides than in the pnictides. This is due to larger Cr-moment for the chalcogenides, which results in larger exchange splitting. This explains the difference in the HM gaps in Figures 1 and 2 for similar lattice parameters.

Figure 3 shows the variation of the magnetic moment with the lattice parameter for the random alloys $CrAs_{50}X_{50}$ (X = Sb, S, Se, Te), where 50% of the As-sublattice is randomly occupied by X-atoms. The

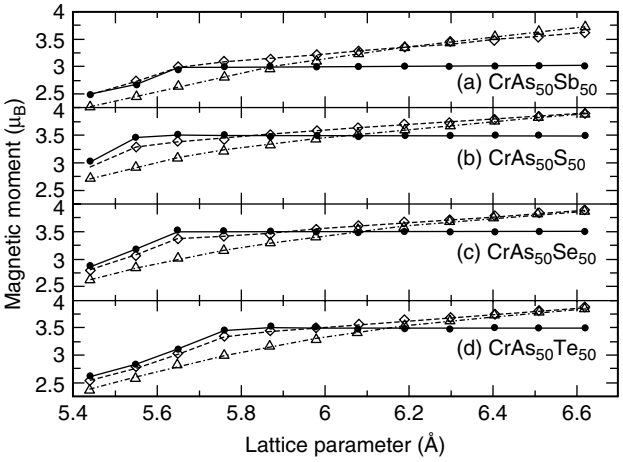

Fig. 3. A comparison of the moment/f.u. with the local Cr moment in the FM state as well as the DLM state for ZB (a) $CrAs_{50}Sb_{50}$, (b) $CrAs_{50}S_{50}$, (c) $CrAs_{50}Se_{50}$, and (d) $CrAs_{50}Te_{50}$. Circle: moment/f.u.- FM state, diamond: local Cr-moment- FM state, triangle: local Cr-moment- DLM state.

saturation moment per f.u. for $CrAs_{50}Sb_{50}$ in the HM state is 3 μB, with the results falling between those for CrAs and CrSb. For $CrAs_{50}X_{50}$ (X = S, Se, Te), the saturation moment per f.u. is 3.5 μB. The local Cr-moment deviates from the saturation value in the HM state, being higher than the saturation value for all lattice parameters above 6.1 Å. Our spin-polarized calculations for the FM reference states lead to local moments not only on the Cr atoms, but also on the other atoms (As, Sb, S, Se, and Te) as well as the empty spheres. The DLM state results are free from such induced moments. The moment per f.u. reaches the saturation values of 4 μB for the pnictides and 3 μB for the chalcogenides in the HM state. The saturation values of the moments for all these alloys satisfy the so-called "rule of 8'': M = (Ztot − 8) μB, where Ztot is the total number of valence electrons in the unit cell (Galanakis and Mavropoulos, 2003). The number 8 accounts for the fact that in the HM state the bonding p bands are full, accommodating 6 electrons, and so is the low-lying band formed of the s electrons from the sp atom, accommodating 2 electrons. The magnetic moment then comes from the remaining electrons filling the d states, first the eg states and then the t2g. The saturation value of 3 μB/f.u., or the HM state, appears for a larger critical lattice constant in CrSb than in CrAs. Similarly, the critical lattice constants for the saturation magnetic moment of 4 μB/f.u. are in increasing order for CrS, CrSe and CrTe.

T_c for CrAs and CrSb ZB alloys and for lattice parameters appropriate to group II–VI and III–V semiconductor substrates, calculated for FM and DLM reference states are shown in Figure 4. Because of uncertainties related to the induced (non-robust) moments on the non-Cr atoms, including empty spheres, for the FM reference states, estimates of Tc for the DLM states should be considered more reliable (Bose and Kudrnovský, 2010). The indicated values clearly point to the possibility of high temperature HM ferromagnetism in these Cr-based pnictides.

Our results are mostly for the ZB structure. However, for CrTe we have carried out additional calculations. Bulk samples of CrTe are known to crystallize in NA structure (Chevreton *et al.,* 1963) with cell parameters $a = 3.997$ Å, $c = 6.222$ Å at room temperature. Both RS and ZB structures are interesting from the standpoint of growing CrTe-films on semiconductor substrates. It is useful to compare the RS and the ZB structure results, because of the different levels of hybridization (even for the same lattice parameter) between the Cr-3d orbital and the sp orbitals of chalcogen/pnictogen atom. We carried out a systematic structural optimization of NA, ZB, and RS CrTe in FM, NM (non-spin polarized) and AFM configurations. For the NA structure, the c/a ratio was optimized and the result c/a = 1.542 for the FM phase is in good agreement with previously obtained result (Ahmadian *et al.,* 2010). This optimized c/a ratio was used for the final NA structure volume optimization. We find the RS phase to be more stable than the ZB phase. Hence we have considered three structures: ZB, RS and NA. Results of energy optimization for these three structures, using the FP-LAPW code (WIEN2k)

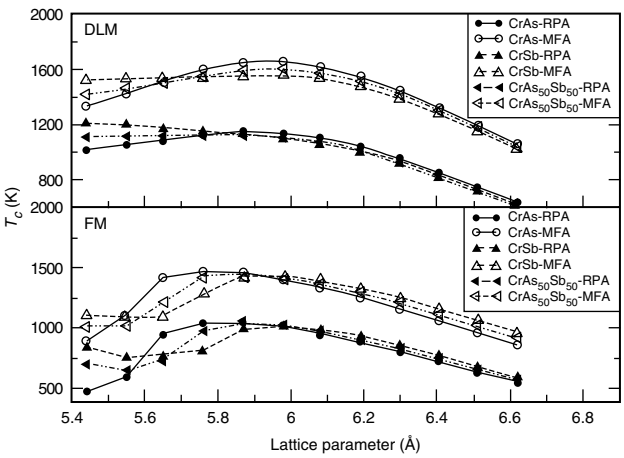

Fig. 4. Curie temperatures in ZB CrAs and CrSb compounds for FM and DLM reference states. For comparison, the results for the mixed alloy $CrAs_{50}Sb_{50}$ are also shown.

and the generalized gradient approximation (GGA) (Perdew *et al*., 1996) are shown in Figure 5. The ZB and RS phases are higher in energies than NA by 0.328 eV and 0.076 eV/atom, respectively. However, the RS structure is only marginally unstable against the NA structure, and more stable than the ZB structure, with an energy that is about 0.25 eV/atom lower. According to our calculation, the ZB phase is more stable than the RS phase for volumes per atom greater than 57 Å^3 (Figure 5). It should be possible to stabilize the RS phase at lower volumes. Recently, Sreenivasan *et al*. and Bi *et al*. were able to grow ZB CrTe films on GaAs substrates (Sreenivasan *et al*., 2008). Their measured values of the lattice parameter lie in the range 6.1–6.21 Å, corresponding to volumes per atom 57–59.9 Å^3. Our calculations suggest that in order to grow RS CrTe one should consider suitable substrates with lattice parameters less than 6.1 or 6.0 Å. For further details, readers should consult our recent publication (Liu *et al.,* 2010). The RS phase is interesting, as it is found to be free from AFM spin fluctuations, which are prevalent in the ZB phase, particularly at low values of the lattice parameter. As a result, the T_c for RS CrTe is higher than that of the ZB phase for all lattice parameters. Preponderance of AFM interactions in the ZB structure for the chalcogenides CrS, CrSe and CrTe at low values of the lattice parameter, is shown in Figure 6. It should be noted that for the pinctides CrAs and CrSb the AFM interactions are much more suppressed.

Figure 7 shows the Cr-Cr exchange interactions in CrAs for both FM and DLM reference states for a wide range of the lattice parameter. Figure 8 shows that for CrTe in the RS structure the Cr-Cr

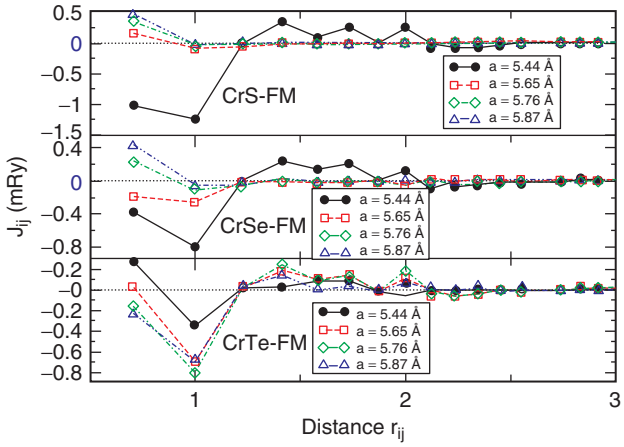

Fig. 6. (Color online) Distance-dependence of the Cr-Cr exchange interaction for the ZB structure Cr-chalcogenides for the FM reference state. The distance between the Cr atoms in Figs. 6–8 is given in units of the lattice parameter *a*.

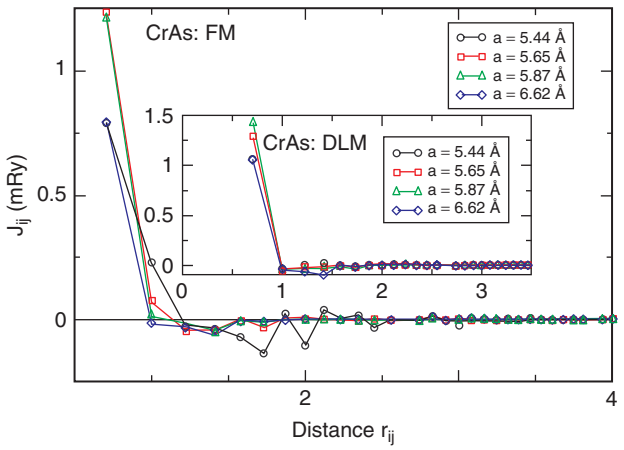

Fig. 7. (Color online) Distance dependence of the exchange interaction between the Cr atoms in CrAs for various lattice parameters *a*, calculated for the FM and DLM reference states.

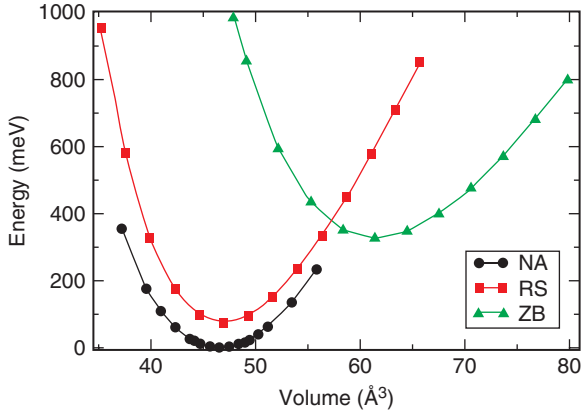

Fig. 5. (Color online) Energy as a function of volume per atom in the three structural phases of CrTe, obtained via FP-LAPW GGA (WIEN2*k*) method.

interactions are entirely FM, whereas for similar lattice parameters or volumes/atom these have a significant AFM component for the ZB phase.

In Figure 9 we compare the Tc^{RPA} values for RS and ZB CrTe, obtained by using the TB-LMTO-Green's function method and using only the exchange interactions between the Cr atoms (strong moments). The reference state used for the calculation is the FM state. For the ZB phase, the use of Eq. (4) of Bose and Kudrnovský (2010) and neglecting all the induced moments results in unphysical negative T_c in the lattice parameter range ~5.7–6.0 Å because of dominant AFM Cr-Cr exchange at the nearest and next nearest neighbor

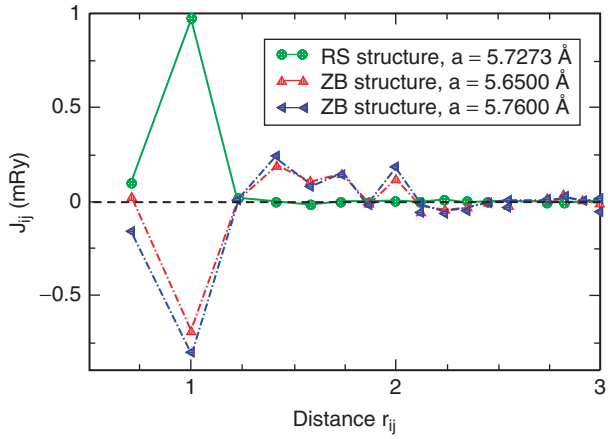

Fig. 8. (Color online) Exchange interaction, computed by using the LMTO-Green's function method, between the Cr atoms in the ZB and RS structure CrTe as a function of the distance. The two lattice parameters for the ZB structure chosen are above and below the equilibrium lattice parameter 5.727 Å; for the RS structure, obtained in the FP-LAPW GGA (WIEN2*k*) calculation.

sites. Since the exchange calculations are done with respect to a 'FM' reference state with parallel magnetic moments, negative values of the exchange interactions, and in particular the exchange constant J0, the sum of the exchange interactions between a Cr-atom and all its neighbours, imply instability of the reference "FM" state.

The ZB phase has been discussed in detail in our previous publication (Bose and Kudrnovský, 2010), where we showed that in spite of these nearest and next nearest neighbor AFM interactions, the FM state is lower in energy than the AFM [001] and AFM [111] states. The cumulative effect of the interactions involving the more distant pairs of Cr atoms, and particularly those due to the induced moments, may stabilize the FM phase. Alternatively, the magnetic state is possibly complex, different from FM, AFM [001] and AFM [111]. If the magnetic state is indeed FM, then according to the prescription of Sandratskii *et al*. T_c should be enhanced with respect to the value given by Eq. (4) and may be positive but small (Sandratskii *et al*., 2007). Note that Sreenivasan *et al*. and Bi *et al*. report the lattice parameters for their ZB CrTe thin films grown on GaAs substrates to be in the range 6.1–6.21 Å and their measurements of remanent magnetization indicate T_c ~100 K. This is not too far off from the calculated values 200–400 K shown in Figure 9. For RS CrTe, on the other hand, all dominant interactions are FM, and as a result the T_c calculated by using Eq. (4) of Bose and Kudrnovský (2010) and based on only Cr–Cr interactions give positive values. The actual T_c s are most probably higher than what is shown in Figure 9.

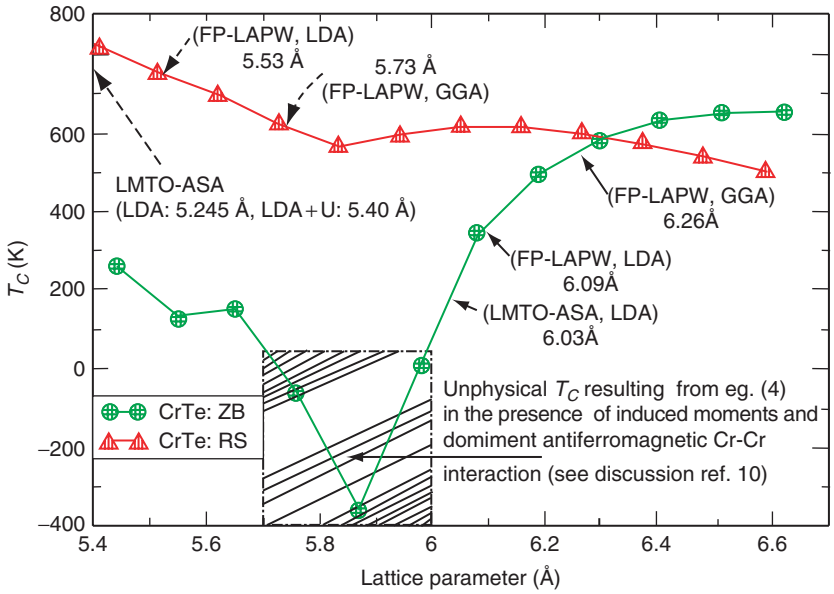

Fig. 9. (Color online) The RPA Curie temperature as a function of the lattice parameter for the ZB and RS structures of CrTe, calculated by considering the Cr-Cr interaction only and by using the FM reference state. The arrows indicate the equilibrium lattice parameter values according to various calculations. The results for T_c are somewhat affected by the 'induced' moments on the Te atoms as well as the empty spheres used in the LMTO Green's function calculation. For ZB CrTe, this error, combined with strong AFM spin fluctuation for the lattice parameters in the range ~5.7–6.0 Å, results in unphysical negative values of T_c in this range. Away from this range T_c values are reliable, although somewhat underestimated.

Magnetism is strongly dependent on the correlation effects. Even though correlation in metallic states is usually well-described within the local density approximation (LDA), different treatments of the exchange and correlation potential may lead to different magnetic moments. The effect of enhanced correlation can be incorporated via the LDA + U method (Anisimov *et al.*, 1997). We find that for CrTe the use of the LDA + U method, with U = 0.075 Ry and J = 0, brings the magnetic moment values in close agreement with those given by GGA in the FP-LAPW method (WIEN2k code). In Figure 10, we compare the T_c values calculated for RS CrTe for the FM reference state, using LDA and LDA + U (with U = 0.075 Ry), and for the DLM reference state using LDA. The results shown use the RPA and up to 111 shells of neighbors to insure convergence of the calculated values. Within the uncertainties of our results there seems to be no appreciable difference between the predictions of LDA and LDA + U.

In Figure 11 we show the Tc values for the mixed pnictide-chalcogenide alloys $CrAs_{50}X_{50}$ (X = S, Se and Te). Because of significant AFM interactions in the chalcogenides for low values of the lattice parameter the FM reference is not ideal for the calculation of T_c in these cases. The preponderance of AFM interactions suggests that the ground state might not be FM for low lattice parameter values. In such cases the DLM state might be closer to the ground state than the FM state. In addition, the presence of induced moments for the FM configuration necessitates the use of multi-sublattice MFA/RPA calculations. In view of that we present results only for the DLM model. The mixed alloy

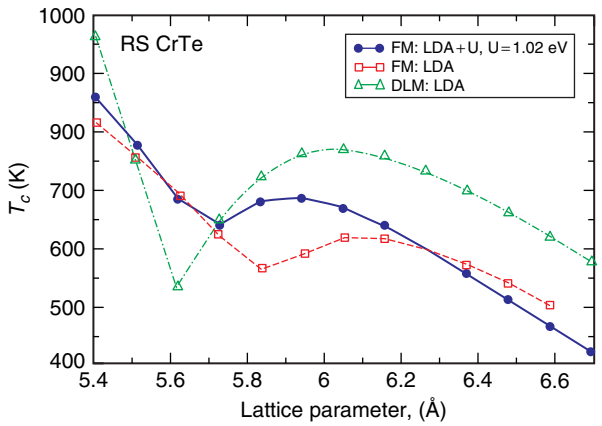

Fig. 10. (Color online) Comparison of the Curie temperature in RS CrTe calculated for the FM reference states in RPA using the LMTO-ASA scheme and LDA and LDA + U methods.

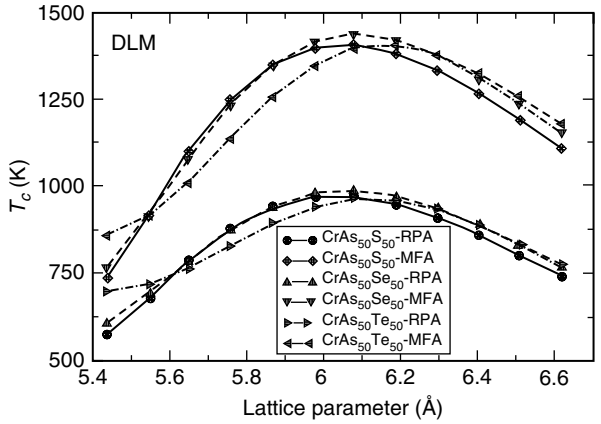

Fig. 11. Variation of Curie temperature as a function of lattice parameters in ZB $CrAs_{50}X_{50}$ alloys with X = S, Se and Te. As can be expected, the results for the Curie temperature in ZB $CrAs_{50}Sb_{50}$ fall, in between those of CrAs and CrSb, as shown in Fig. 4. All results shown are for DLM reference states, and as such, should be considered as upper limits for T_c.

cases are interesting to study in as much as they provide some flexibility in the manipulation of the lattice parameter via concentration variation. Note that the RPA values are lower as well as more reliable estimates of T_c than those given by MFA, which is known to significantly overestimate the Curie temperature.

4. Conclusions

Our ab initio studies of the electronic structure, magnetic moments, exchange interactions and Curie temperatures in ZB CrX (X = As, Sb, S, Se and Te) and $CrAs_{50}X_{50}$ (X = Sb, S, Se and Te) reveal that half-metallicity in these alloys is maintained over a wide range of lattice parameters. The results for the exchange interaction and the Curie temperature show that these alloys have relatively high Curie temperatures, i.e. room temperature and above. The exceptions occur for the alloys involving S, Se and Te at some low values of lattice parameters, where significant inter-atomic AFM exchange interactions indicate ground states to be either AFM or of a complex magnetic nature. Our results for the Curie temperature, the lattice Fourier transform of the exchange interactions, and the resulting stability analysis are based on the exchange interactions between the Cr atoms only. Because our method yields induced magnetic moments on the non-Cr atoms, including some of the empty spheres, the results for T_c and the lattice Fourier transforms contain some errors. However, since the Cr-moments and the

Cr-Cr exchange interactions are by far the strongest ones, the errors should be small enough to provide qualitative insights to experimentalists in the field. For the purpose of the lattice matching with a given substrate, one can resort to alloying on the non-Cr sublattice, combining pnictogens with chalcogen atoms. As long as the concentration of the pnictogens is higher than that of the chalcogens, the FM state in the ZB structure should be a stable half-metal with a relatively large value of T_c.

For the chalcogenide CrTe we have explored the relative stability of ZB and RS structures. Although the ground state of this compound is NA, at high values of volume/atom the ZB structure has lower energy. In addition, for some range of the lattice parameter (Figure 5) the RS structure is more stable than ZB. In the RS phase CrTe is free from AFM interactions. According to our results, the chalcogenide CrTe should be stable in the RS phase at lattice parameters less than 6.1 Å, and should exhibit HM- FM behavior with relatively high T_c.

Future work in this regard, some of which is already in progress, should involve a systematic comparative study of stability, ferromagnetism and half-metallicity in all of the Cr-based chalcogenides and pnictides.

Acknowledgments

This work was supported by a grant from the Natural Sciences and Engineering Research Council of Canada. J.K. acknowledges financial support from AV0Z 10100520 and the Czech Science Foundation (202/09/0775)

References

Ahmadian F., Abolhassani M.R., Hashemifar S.J. and Elahi M., 2010. Robust half-metallicity at the zincblende CrTe (001) surfaces and its interface with ZnTe (001). *J. Magn. Magn. Mater.* **322(8)**, 1004–1014.

Akinaga H., Manago T. and Shirai M., 2000. Material design of half-metallic zinc-blende CrAs and the synthesis by molecular-beam epitaxy. *Jpn. J. Appl. Phys.* **39**, 1118–1120.

Andersen O.K. and Jepsen O., 1984. Explicit, first-principles tight-binding theory. *Phys. Rev. Lett.* **53(27)**, 2571–2574.

Anisimov V.I., Aryasetiawan F. and Lichtenstein A.I., 1997. First-principles calculations of the electronic structure and spectra of strongly correlated systems: the LDA + *U* method. *J. Phys.: Condens. Matter* **9(4)**, 767–808.

Bi J.F., Sreenivasan M.G., Teo K.L. and Liew T., 2008. Observation of strong magnetic anisotropy in zinc-blende CrTe thin films. *J. Phys. D: Appl. Phys.* **41(4)**, 21–24.

Blaha P., Schwarz K.G., Madsen K. H., Kvasnicka D. and Luitz J., 2001. WIEN2*k*, An Augmented-Plane-Wave-local Orbitals Program for Calculating Crystal Properties, Tech.nische Universitaet Wien, Austria.

Bose S.K., Kudrnovský J., 2010. Exchange interactions and curie temperatures in Cr-based alloys in the zinc blende structure: Volume-and composition-dependence from first-principles calculations. *Phys. Rev. B* **81(5)**, 1–16.

Chevreton M., Bertaut E.F. and Jellinek F., 1963. Quelques remarques surle systeme Cr–Te. *Acta Crystallogr.* **16(5)**, 431.

Deng J.J., Zhao J.H., Bi J. F., Niu Z.C., Yang F.H., Wu X.G. and Zheng H. Z., 2006. Growth of thicker zinc-blende CrSb layers by using (In, Ga) As buffer layers. *J. Appl. Phys.* **99(9)**, 21–23.

Galanakis I. and Mavropoulos P., 2003. Zinc-blende compounds of transition elements with N, P, As, Sb, S, Se, and Te as half-metallic systems. *Phys. Rev. B* **67(10)**, 71–78.

Heine V., 1980. Electronic structure from the point of view of the local atomic environment. *Solid State Physics* **35**, 1–127.

Kudrnovský J. and Drchal V., 1990. Electronic structure of random alloys by the linear band-structure methods. *Phys. Rev. B* **41(11)**, 515–528.

Liu Y., Bose S.K. and Kudrnovský J., 2010. First-principles theoretical studies of half-metallic ferromagnetism in CrTe. *Phys. Rev. B* **82(9)**, 351–358.

Perdew J.P., Burke K. and Ernzerhof M., 1996. Generalized gradient approximation made simple. *Phys. Rev. Lett.* **77(18)**, 3865–3868.

Saito, H., Zayets V., Yamagata S. and Ando K., 2003. Room-temperature ferromagnetism in a II–VI diluted magnetic semiconductor Zn_{1-x} Cr_x Te. *Phys. Rev. Let.* **90(20)**, 21–24.

Sandratskii L.M., Singer R. and Sasioğlu E., 2007. Heisenberg Hamiltonian description of multiple-sublattice itinerant-electron systems: general considerations and applications to NiMnSb and MnAs. *Phys. Rev. B* **76 (18)**, 406–420.

Savrasov S.Yu. and Savrasov D.Yu., 1992. Full-potential linear-muffin-tin-orbital method for calculating total energies and forces. *Phys. Rev. B* **46(19)**, 181–195.

Sreenivasan M.G., Bi J.F., Teo K.L. and Liew T., 2008. Systematic investigation of structural and magnetic properties in molecular beam epitaxial growth of metastable zinc-blende CrTe toward half-metallicity. *J. Appl. Phys.* **103(4)** 908–913.

Vosko S.H., Wilk L. and Nusair M., 1980. Accurate spin-dependent electron liquid correlation energies for local spin density calculations: a critical analysis. *Can. J. Phys.* **58(8)**, 1200–1211.

Zhao J.H., Matsukura F., Takamura K., Abe E., Chiba D. and Ohno H., 2001. Room-temperature ferromagnetism in zincblende CrSb grown by molecular-beam epitaxy. *Appl. Phys. Lett.* **79(17)**, 76–79.